POLISH MARITIME RESEARCH 1(64) 2010 Vol 17; pp. 3-9
10.2478/v10012-008-0059-8

Numerical analysis of influence of ship hull form modification on ship resistance and propulsion characteristics

Part II
Influence of hull form modification on wake current behind the ship

Tomasz Abramowski, Ph. D.
Tadeusz Szelangiewicz, Prof.
West Pomeranian University of Technology, Szczecin

ABSTRACT

After signing ship building contract shipyard's design office orders performance of ship resistance and propulsion model tests aimed at, apart from resistance measurements, also determination of ship speed, propeller rotational speed and propulsion engine power for the designed ship, as well as improvement of its hull form, if necessary. Range of ship hull modifications is practically very limited due to cost and time reasons. Hence numerical methods, mainly CFD ones are more and more often used for such tests. In this paper consisted of three parts, are presented results of numerical calculations of hull resistance, wake and efficiency of propeller operating in non-homogenous velocity field, performed for research on 18 hull versions of B573 ship designed and built by Szczecin Nowa Shipyard.

Keywords: ship hull geometry, numerical (computational) fluid dynamics, resistance, wake, propeller efficiency

NUMERICAL COMPUTATIONS OF WAKE CURRENT

The second effect of ship hull form modification, apart from change of resistance, is change of wake current which to a large extent influences performance of screw propeller (its thrust, torque and efficiency) as well as overall propulsive efficiency of ship.

Before commencing actual numerical computations a comparative test has been performed, namely, for the initial hull form of B 573 ship wake current has been numerically calculated and obtained results compared with its model tests.

Comparative test for wake current computations

Ship draught T = 11.3 [m]
Water density $\rho = 999.0$ [$kg \cdot m^3$]
Kinematic viscosity $\nu = 1.13896$ [$m^2 \cdot s^1$]

Wake fractions were determined in compliance with the axial component velocity V_x, according to the relation:

$$W_X = 1 - \frac{V_X}{V_M} \qquad (2)$$

The computation results are presented graphically in Fig. 13 ÷ 16, and numerically - in Tab. 5. In Tab. 6 the results of model tests [1] are given for comparison. The average value of wake fraction determined numerically within the range of values of the relative propeller radius r/R reaching from 0.25 to 1.21 is equal to 0.48, while that obtained from the model tests amounts to 0.52.

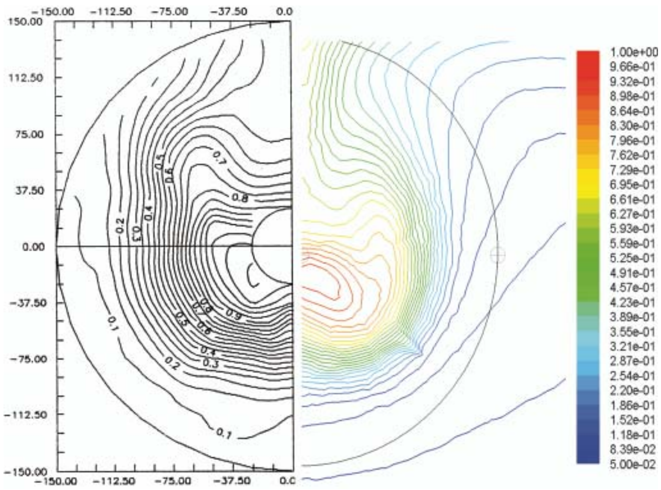

Fig. 13. Axial wake fraction distribution on the propeller disk plane: on the right side – results of the numerical test, on the left side – results of the model test [1]

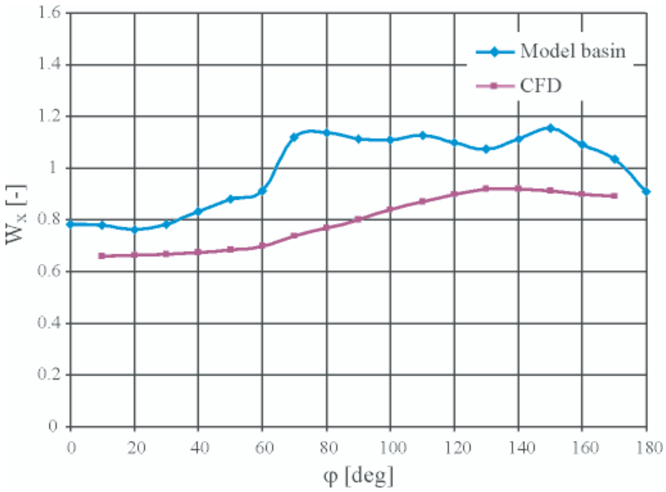

***Fig. 14.** Circumferential distribution of axial wake fraction component for r/R = 0.202*

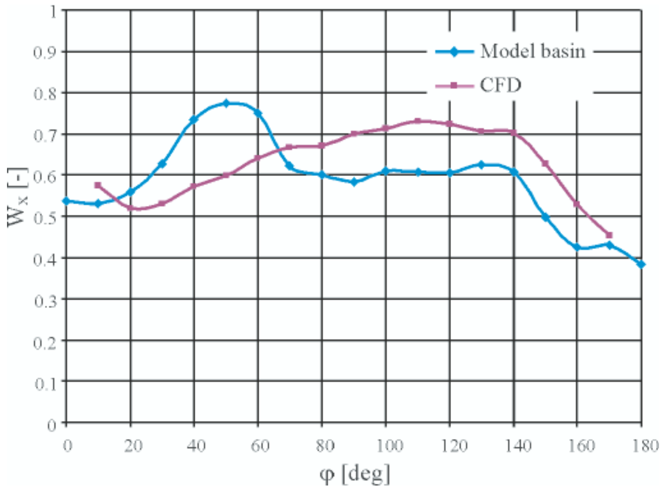

***Fig. 15.** Circumferential distribution of axial wake fraction component for r/R = 0.60*

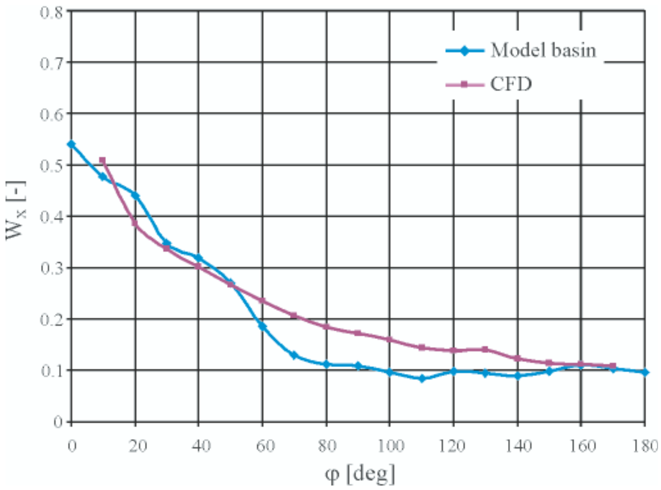

***Fig. 16.** Circumferential distribution of axial wake fraction component for r/R = 1.0*

In Fig. 17 stream lines for the inital ship hull form are also shown.

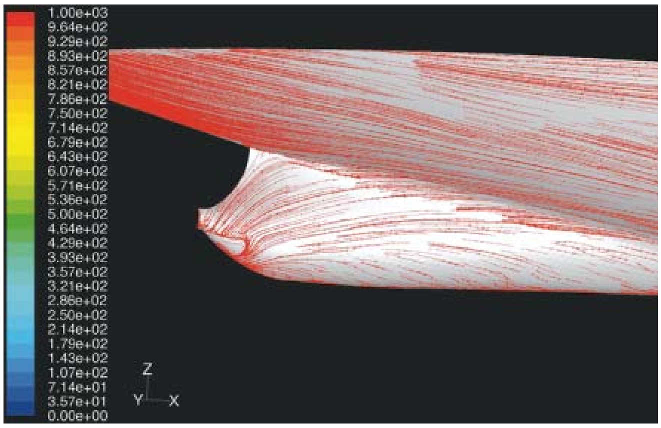

***Fig. 17.** Distribution of stream lines on ship hull model*

Tab. 5. Results of numerical calculations of the axial wake fraction component W_x [-]

r [mm]	25	37.5	50	62.5	75	87.5	100	112.5	125	137.5	150
φ [deg]											
10	0.6595	0.6383	0.6212	0.5977	0.5746	0.5451	0.521	0.5108	0.5094	0.5092	0.5389
20	0.6627	0.6353	0.5994	0.5658	0.52	0.4793	0.4383	0.4079	0.3853	0.3747	0.3787
30	0.6663	0.6316	0.6004	0.5676	0.5306	0.4839	0.4268	0.3783	0.337	0.3139	0.3028
40	0.6738	0.6365	0.615	0.5968	0.572	0.507	0.427	0.3485	0.3015	0.2709	0.2562
50	0.6843	0.6476	0.6449	0.6427	0.5997	0.5153	0.4162	0.3163	0.266	0.2385	0.2195
60	0.6998	0.674	0.6692	0.6786	0.6395	0.5285	0.3882	0.2989	0.2355	0.2072	0.1906
70	0.7364	0.6949	0.702	0.7093	0.6676	0.5308	0.3962	0.262	0.2073	0.1817	0.1677
80	0.7674	0.7267	0.7221	0.7351	0.6703	0.5154	0.3919	0.2507	0.1838	0.1636	0.1488
90	0.8005	0.7552	0.7469	0.7587	0.7001	0.5467	0.3797	0.2505	0.1715	0.1467	0.1347
100	0.8391	0.804	0.7794	0.781	0.7121	0.566	0.3707	0.2258	0.1601	0.1344	0.1225
110	0.871	0.8441	0.8131	0.7976	0.7299	0.5715	0.3586	0.2128	0.1436	0.1236	0.113
120	0.8992	0.8773	0.8404	0.8161	0.7236	0.5745	0.3484	0.1958	0.1391	0.1158	0.1053
130	0.9197	0.9042	0.8653	0.8176	0.7064	0.5448	0.3567	0.2119	0.1397	0.1101	0.0992
140	0.9204	0.9083	0.8645	0.8055	0.7012	0.4911	0.2737	0.1681	0.1227	0.1033	0.0943
150	0.9114	0.8791	0.8406	0.7467	0.6279	0.4252	0.254	0.1511	0.1143	0.1001	0.0909
160	0.8998	0.8588	0.8035	0.7018	0.5283	0.3518	0.2067	0.1414	0.1122	0.0989	0.0897
170	0.8927	0.8361	0.7455	0.6106	0.4542	0.2885	0.18	0.129	0.1088	0.0969	0.088

Tab.6. *Results of model tests of the axial wake fraction component* W_x *[-]*

r/R	0.202	0.25	0.3	0.35	0.4	0.5	0.6	0.7	0.8	0.9	0.95	1	1.21
r [mm]	**25**	**31**	**37.2**	**43.4**	**49.6**	**62**	**74.4**	**86.8**	**99.2**	**111.6**	**117.8**	**124**	**150**
φ [deg]													
0	0.783	0.736	0.692	0.652	0.617	0.566	0.537	0.531	0.535	0.537	0.538	0.540	0.570
10	0.778	0.731	0.686	0.646	0.612	0.562	0.531	0.516	0.506	0.492	0.484	0.478	0.466
20	0.763	0.715	0.671	0.633	0.604	0.570	0.559	0.551	0.526	0.485	0.463	0.440	0.359
30	0.784	0.741	0.702	0.670	0.646	0.626	0.628	0.611	0.537	0.433	0.387	0.348	0.250
40	0.830	0.797	0.767	0.744	0.727	0.718	0.734	0.702	0.583	0.432	0.369	0.319	0.197
50	0.881	0.857	0.835	0.816	0.801	0.785	0.774	0.701	0.552	0.389	0.323	0.270	0.152
60	0.913	0.893	0.874	0.856	0.840	0.807	0.750	0.630	0.458	0.294	0.232	0.186	0.116
70	1.119	1.121	1.105	1.068	1.005	0.814	0.623	0.458	0.312	0.198	0.157	0.130	0.111
80	1.138	1.141	1.122	1.079	1.006	0.789	0.600	0.438	0.291	0.177	0.138	0.112	0.104
90	1.111	1.113	1.098	1.063	1.005	0.817	0.584	0.391	0.253	0.157	0.126	0.108	0.111
100	1.108	1.109	1.095	1.061	1.005	0.824	0.610	0.423	0.271	0.157	0.119	0.097	0.112
110	1.127	1.130	1.113	1.073	1.005	0.802	0.608	0.438	0.281	0.155	0.112	0.084	0.087
120	1.099	1.101	1.088	1.057	1.004	0.832	0.605	0.408	0.263	0.157	0.121	0.098	0.089
130	1.073	1.074	1.065	1.042	1.003	0.865	0.626	0.415	0.266	0.153	0.116	0.094	0.104
140	1.112	1.114	1.099	1.064	1.005	0.819	0.607	0.422	0.271	0.155	0.115	0.089	0.083
150	1.156	1.159	1.138	1.089	1.007	0.754	0.498	0.302	0.182	0.124	0.109	0.099	0.088
160	1.090	1.080	1.049	0.991	0.902	0.650	0.426	0.263	0.167	0.128	0.118	0.110	0.091
170	1.034	1.018	0.985	0.932	0.856	0.643	0.429	0.261	0.161	0.121	0.111	0.103	0.079
180	0.909	0.876	0.834	0.783	0.721	0.565	0.383	0.226	0.134	0.103	0.098	0.096	0.079

RESULTS OF ANALYSIS OF WAKE CURRENT FOR MODIFIED VERSIONS OF SHIP HULL

Numerical calculations of wake current were performed for the same modified ship hull versions as in the case of the resistance investigations (Tab. 2).

The ship hull model speed V = 1.492 [m/s].

The collected results of numerical calculations in the form of the average wake fraction according to Eq. (2), are given in Tab. 7.

The influence of particular modified geometrical parameters of ship hull model on the average value of wake fraction is presented in Figs. 18 ÷ 20, and, in Fig. 21 and 22 are given circumferential distributions of axial and tangential wake fraction components for r/R = 0,6.

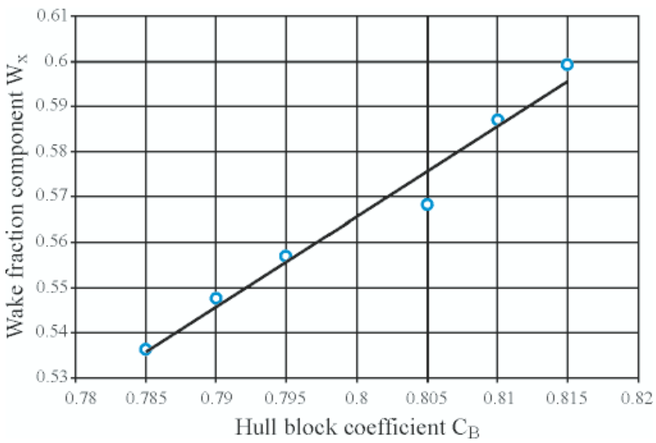

Fig. 18. *Wake fraction component* W_x *calculated in function of* C_B

Tab. 7. *Average values of axial wake fraction for modified hull versions of B 573 ship*

Number of variant	Modified parameter	Average value of axial wake fraction
	C_B	W_x
1	0.79	0.547
2	0.795	0.556
3	0.785	0.536
4	0.81	0.586
5	0.805	0.568
6	0.815	0.599
	C_P	
7	0.78	0.539
8	0.77	0.523
9	0.76	0.507
10	0.8	0.578
11	0.81	0.602
	LCB	
12	47%	0.517
13	46%	0.491
14	45%	0.468
15	49%	0.593
16	50%	0.620
17	51%	0.681
18	Manual modification	0.471

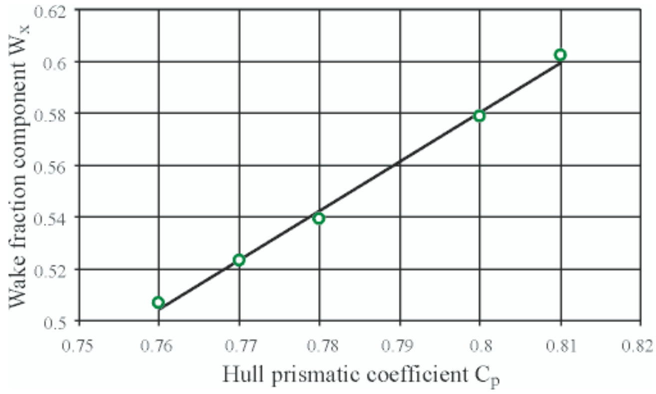

Fig. 19. *Wake fraction component W_x calculated in function of C_P*

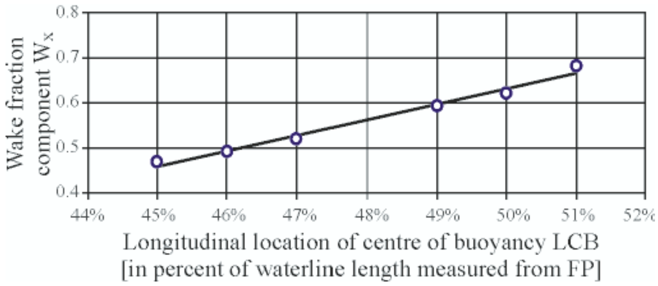

Fig. 20. *Wake fraction component W_x calculated in function of LCB*

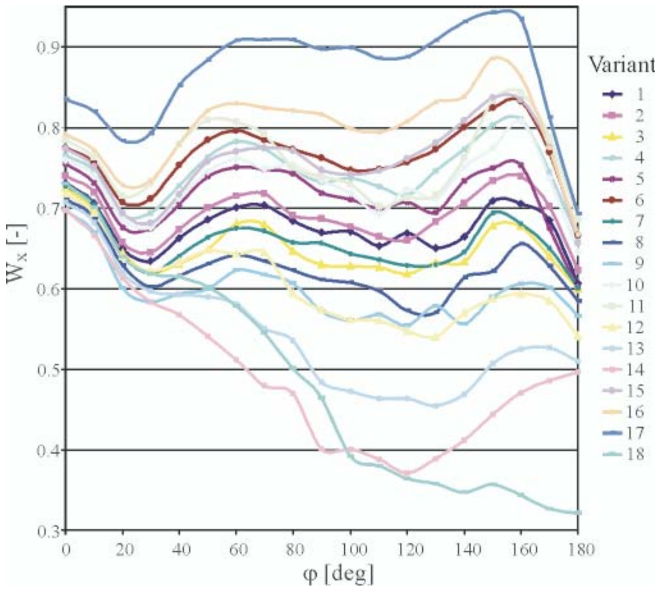

Fig. 21. *Circumferential distribution of field of the axial wake fraction component for r/R = 0.6, calculated for all the analyzed variants (18 in number)*

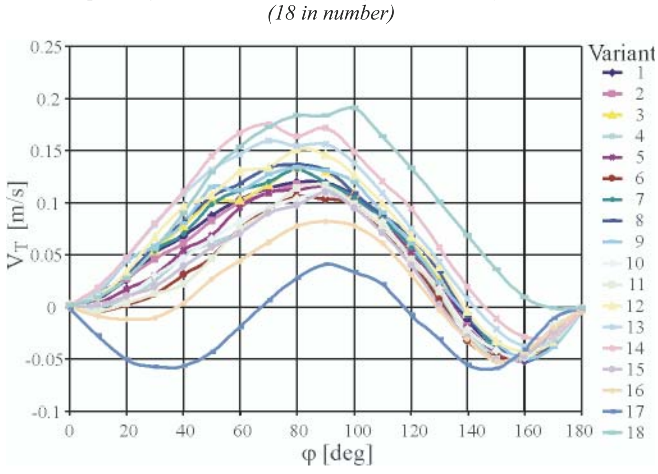

Fig. 22. *Circumferential distribution of field of the tangential velocity component for r/R = 0.6, calculated for all the analyzed variants (18 in number)*

In Figs. 23 ÷ 29 are exemplified distributions of tangential and axial wake fractions as well as velocity vectors on the propeller disk plane for selected variants of B 573 ship hull modification.The complete set of numerical calculation results is contained in the report on the research project [2].

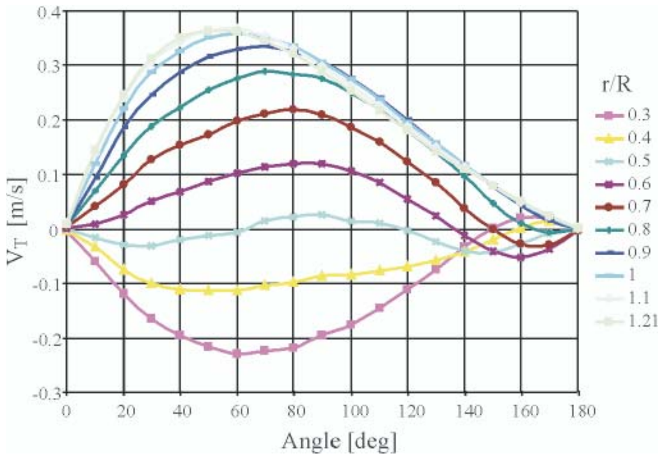

Distribution of the tangential velocity V_T

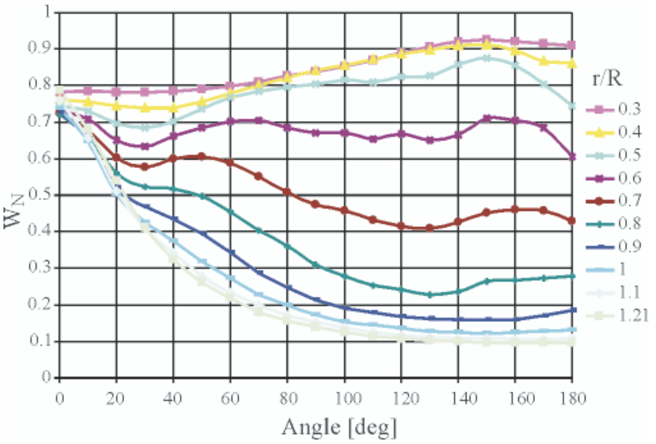

Distribution of the axial wake fraction component W_N

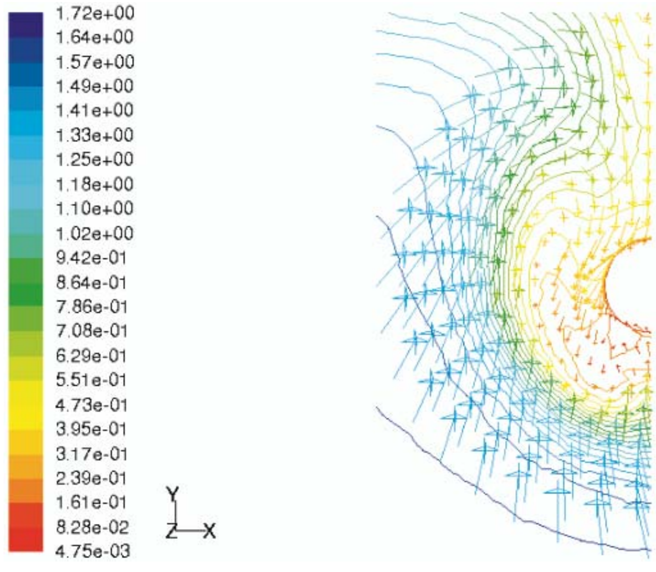

Wake current velocity vectors

Fig. 23. *Distributions of tangential velocities and axial wake fraction as well as velocity vectors in propeller disk plane for variant 1 of B 573 ship hull modification*

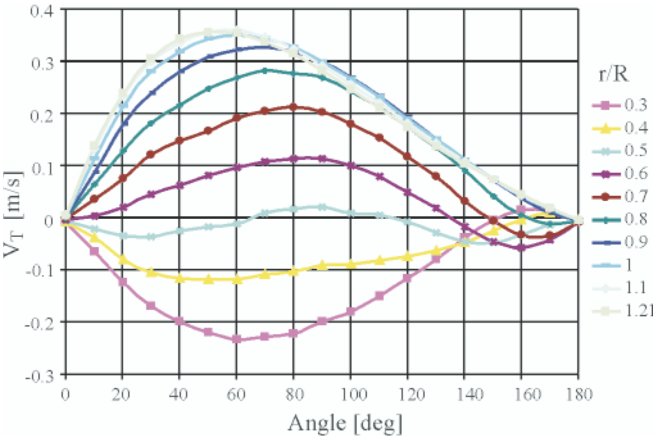

Distribution of the tangential velocity V_T

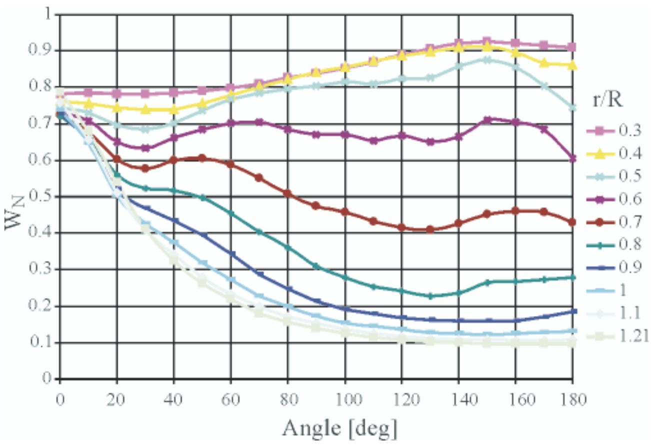

Distribution of the axial wake fraction component W_N

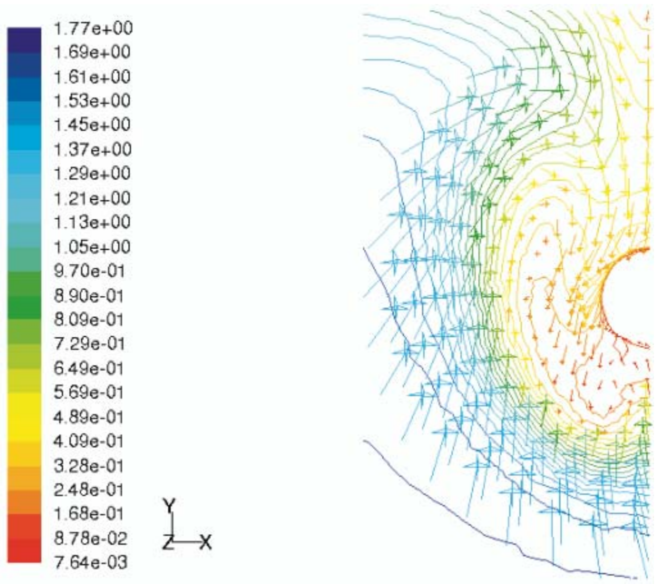

Wake current velocity vectors

Fig. 24. *Distributions of tangential velocities and axial wake fraction as well as velocity vectors on propeller disk plane for variant 6 of B 573 ship hull modification*

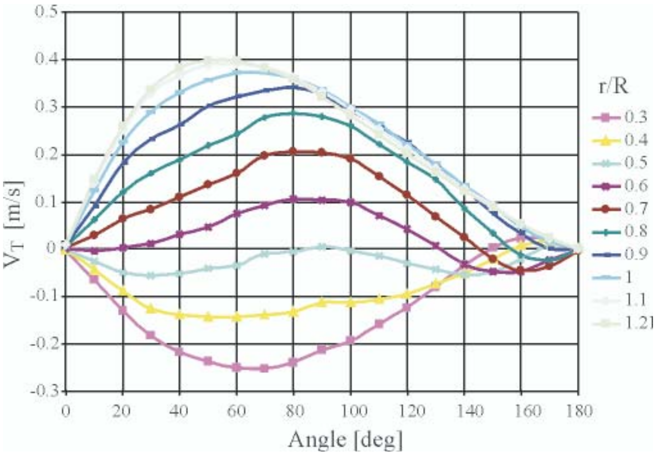

Distribution of the tangential velocity V_T

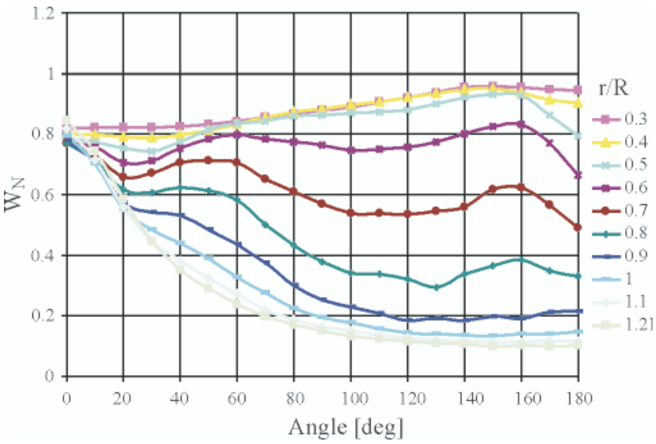

Distribution of the axial wake fraction component W_N

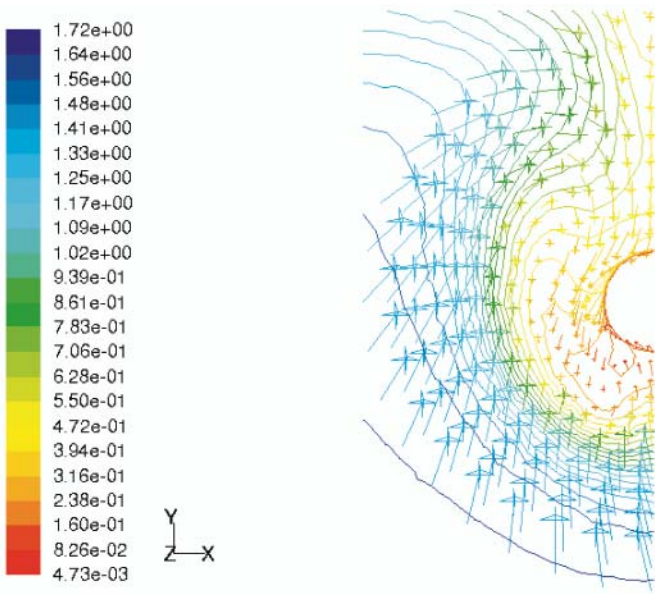

Wake current velocity vectors

Fig. 25. *Distributions of tangential velocities and axial wake fraction as well as velocity vectors on propeller disk plane for variant 7 of B 573 ship hull modification*

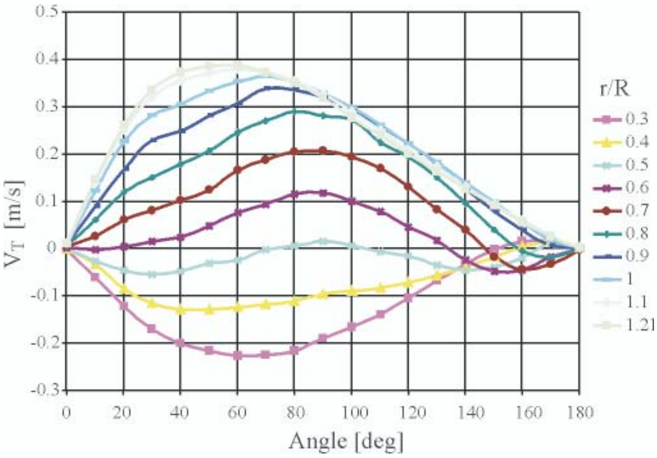

Distribution of the tangential velocity V_T

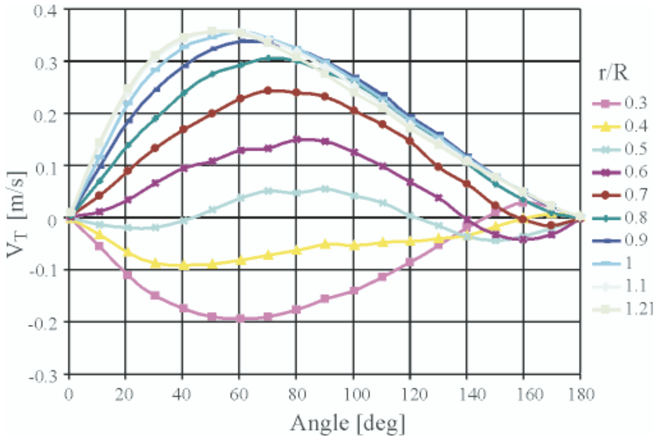

Distribution of the tangential velocity V_T

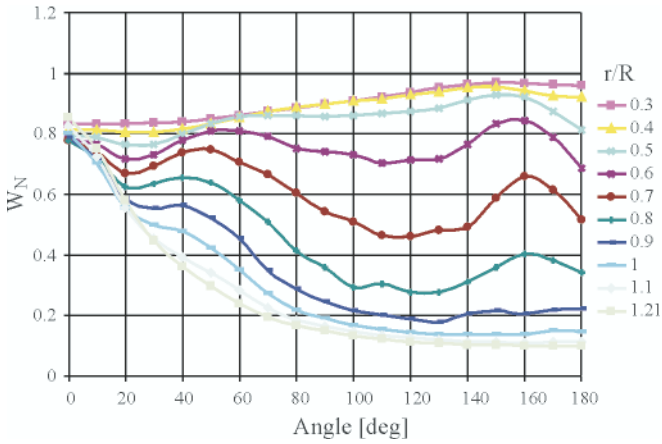

Distribution of the axial wake fraction component W_N

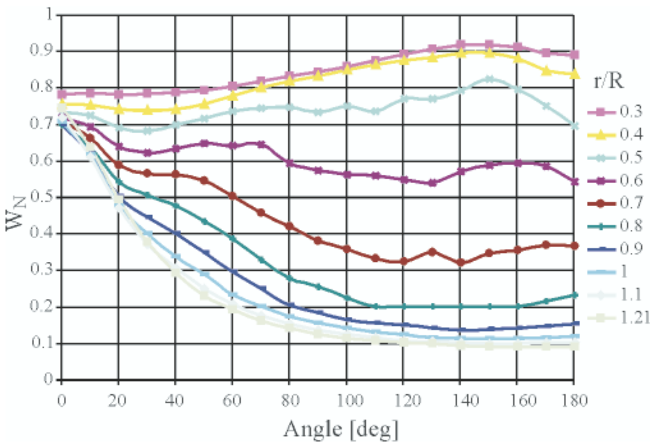

Distribution of the axial wake fraction component W_N

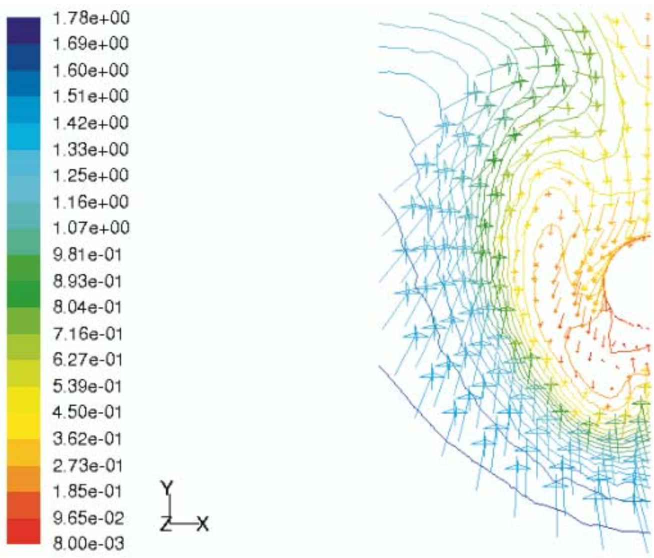

Wake current velocity vectors

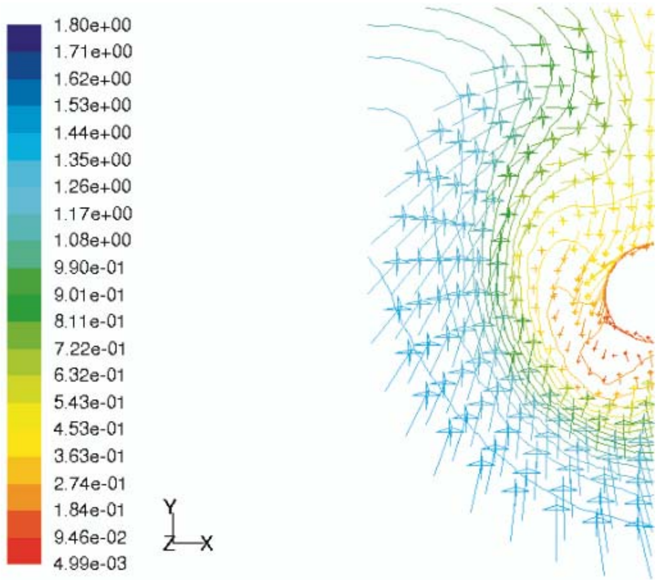

Wake current velocity vectors

Fig. 26. *Distributions of tangential velocities and axial wake fraction as well as velocity vectors on propeller disk plane for variant 11 of B 573 ship hull modification*

Fig. 27. *Distributions of tangential velocities and axial wake fraction as well as velocity vectors on propeller disk plane for variant 12 of B 573 ship hull modification*

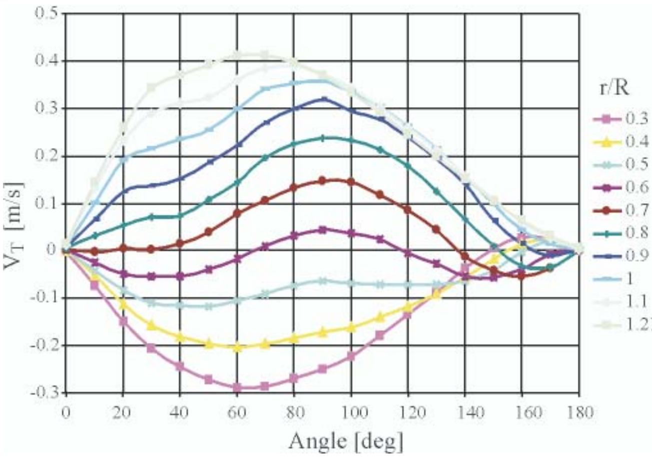

Distribution of the tangential velocity V_T

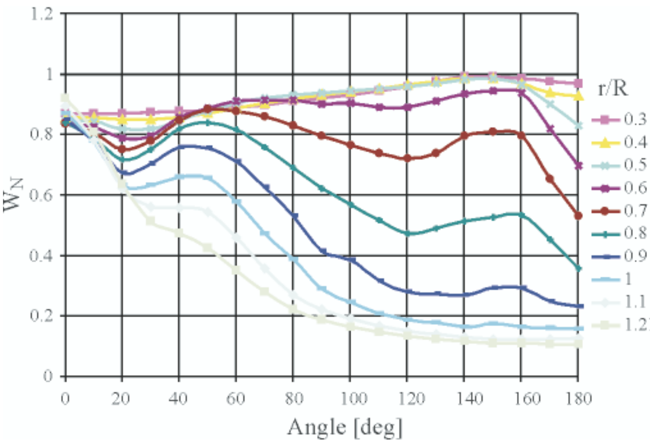

Distribution of the axial wake fraction component W_N

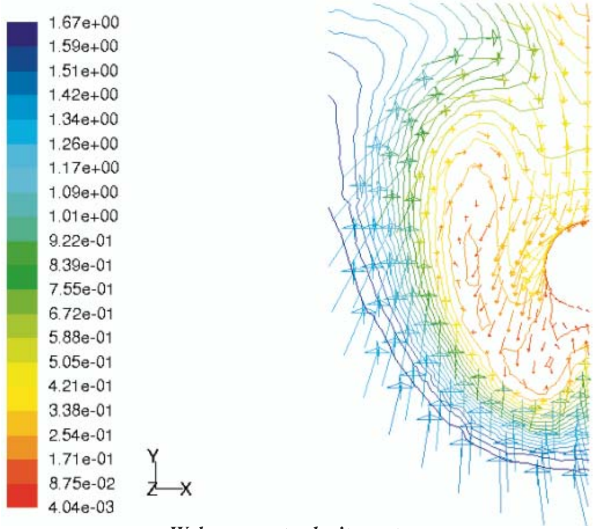

Wake current velocity vectors

Fig. 28. *Distributions of tangential velocities and axial wake fraction as well as velocity vectors on propeller disk plane for variant 17 of B 573 ship hull modification*

Acknowledgements

Results of the investigations presented in this paper have been financed by Ministry of Science and Higher Education in the frame of the research project no. R10 008 01.

BIBLIOGRAPHY

1. Jaworski S., Syrocki W.: *Ship B 573: Results of Model Tests - Resistance, Wake Measurements*, Technical Report No. RH-95/ T-041A, Ship Design and Research Centre, Gdańsk, 1995
2. Szelangiewicz T.: *Numerical investigations on ship rudder-propeller -stern co-operation aimed at the improving of*

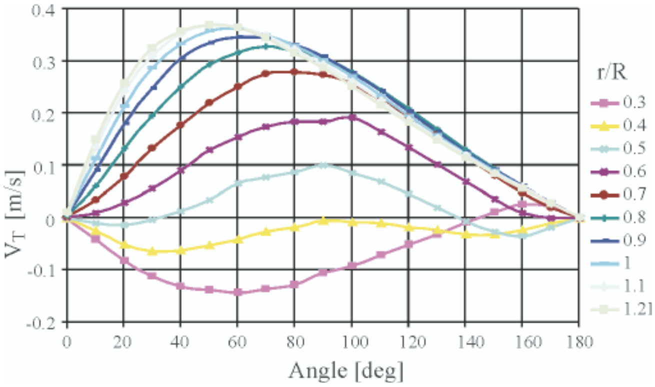

Distribution of the tangential velocity V_T

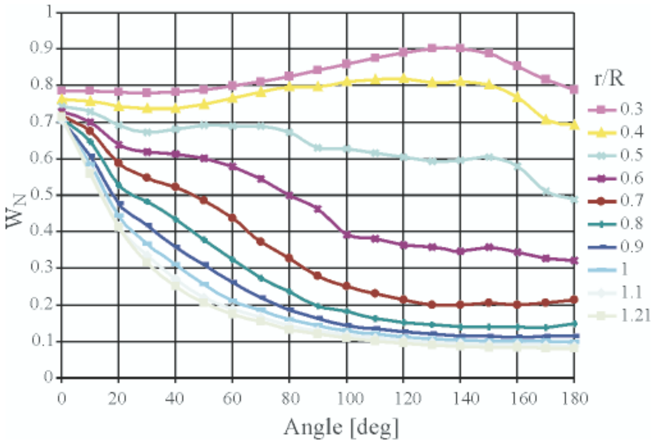

Distribution of the axial wake fraction component W_N

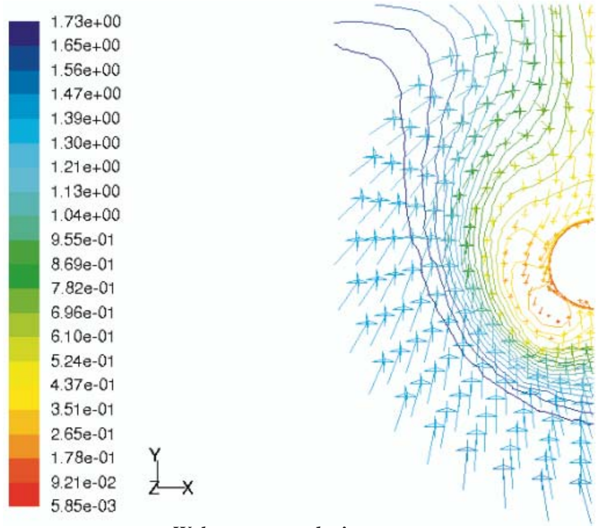

Wake current velocity vectors

Fig. 29. *Distributions of tangential velocities and axial wake fraction as well as velocity vectors on propeller disk plane for variant 18 of B 573 ship hull modification*

transport ship propulsion and maneouvrability properties (in Polish). Appendix to the final report on realization of the development project No. R 10 008 01, Szczecin 2009.

CONTACT WITH THE AUTHORS

Tomasz Abramowski, Ph. D.
Tadeusz Szelangiewicz, Prof.
West Pomeranian University of Technology, Szczecin
Faculty of Marine Technology
Al. Piastów 41
71-065 Szczecin, POLAND
e-mail: tadeusz.szelangiewicz@ps.pl